This is an open access article published under an ACS AuthorChoice License, which permits copying and redistribution of the article or any adaptations for non-commercial purposes.

ACS OMEGA

http://pubs.acs.org/journal/acsodf

Article

Efficient and Straightforward Syntheses of Two United States Pharmacopeia Sitagliptin Impurities: 3-Desamino-2,3-dehydrositagliptin and 3-Desamino-3,4-dehydrositagliptin

Matej Sova,[§] Rok Frlan,[§] Stanislav Gobec, and Zdenko Časar*

Cite This: *ACS Omega* 2020, 5, 5356−5364

Read Online

ACCESS | Metrics & More | Article Recommendations | Supporting Information

ABSTRACT: Various organic impurities (starting materials, reagents, intermediates, degradation products, by-products, and side products) could be present in active pharmaceutical ingredients affecting their qualities, safeties, and efficacies. Herein, we present the efficient syntheses of two United States Pharmacopeia impurities of an antidiabetic drug sitagliptin, a potent and orally active dipeptidyl peptidase IV inhibitor: 3-desamino-2,3-dehydrositagliptin and 3-desamino-3,4-dehydrositagliptin. Our three-step synthetic approach is based on the efficient cobalt-catalyzed cross-coupling reaction of 1-bromo-2,4,5-trifluorobenzene and methyl 4-bromocrotonate in the first step, followed by hydrolysis of corresponding ester with 3 M HCl to (*E*)-(2,4,5-trifluorophenyl)but-2-enoic acid in high overall yield, whereas the reaction with 3 M NaOH resulted in the carbon−carbon double bond regio-isomerization and hydrolysis to give the (*E*)-(2,4,5-trifluorophenyl)but-3-enoic acid in 92% yield. Both acid derivatives were converted to title compounds via the amide bond formation with 3-(trifluoromethyl)-5,6,7,8-tetrahydro-[1,2,4]triazolo[4,3-*a*]pyrazine. Extensive screening of coupling/activation reagents, bases, and solvents reviled that the amide bond is formed the most efficiently using the $(COCl)_2/Et_3N$ in THF or alternatively EDC/NMM/(DMAP or HOBt) in DMF obtaining the title compounds in 68−76% yields and providing the overall yields for the three-step process in the range of 57−64% on a gram scale. The presented study also demonstrates the importance of a proper selection of solvent, base, and coupling/activating reagent for amide bond formation using Michael acceptor-type allylbenzene derivatives as coupling partners to minimize the carbon−carbon double bond regio-isomerization.

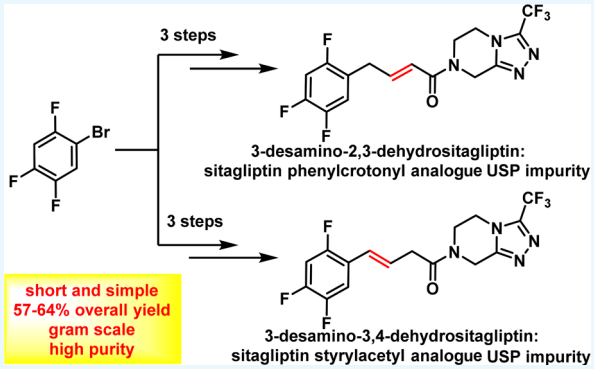

INTRODUCTION

Sitagliptin ((3*R*)-3-amino-1-(3-(trifluoromethyl)-5,6-dihydro-[1,2,4]triazolo[4,3-*a*]pyrazin-7(8*H*)-yl)-4-(2,4,5-trifluorophenyl)butan-1-one (**1**), Figure 1) is a potent and orally active dipeptidyl peptidase IV (DPP-4) inhibitor discovered by Merck.[1] After the approval by FDA in 2006, it has been used for the treatment of diabetes mellitus type 2 under the brand name Januvia.[2] Sitagliptin is the most important drug in the class of DPP-4 inhibitors or even among antidiabetes drugs overall with a market value of more than US$ 11.4 billion in 2018 (US$ 7.5 billion for monoproduct and US$ 3.9 billion for fixed-dose combination with metformin; IQVIA Analytics Link data).

The majority of active pharmaceutical ingredients (APIs) are produced by organic syntheses; therefore, various organic impurities such as starting materials, reagents, intermediates, by-products, and side products could be present in the API. Furthermore, some impurities are also formed during the degradation process under storage conditions.[3] Impurity profile studies are thus essential to ensure purity, quality, safety, and efficacy during API development.[3−5] In the case of sitagliptin, small quantities of degradation impurities or related substances may have an impact on its antidiabetic activity and may be potentially toxic. Therefore, based on the value of sitagliptin in diabetes treatment, it is of huge importance that the quality of the drug is properly controlled using high quality analytical standards of impurities.[5m] Up to date, several structurally diverse impurities of sitagliptin were reported in the literature and pharmacopeia (Figure 1)[4,6−8] such as the 1-phenylethyl derivative of sitagliptin **2** and 3-(trifluoromethyl)-5,6,7,8-tetrahydro-[1,2,4]triazolo[4,3-*a*]pyrazine (**3**) as intermediates in the manufacturing process, a recently reported 1-cyclohexylethyl derivative of sitagliptin **4** and enantiomer impurity **5**, which are side reaction products generated during the catalytic hydrogenation in the final step of sitagliptin

Received: December 20, 2019
Accepted: February 13, 2020
Published: March 3, 2020

© 2020 American Chemical Society

https://dx.doi.org/10.1021/acsomega.9b04393
ACS Omega 2020, 5, 5356−5364

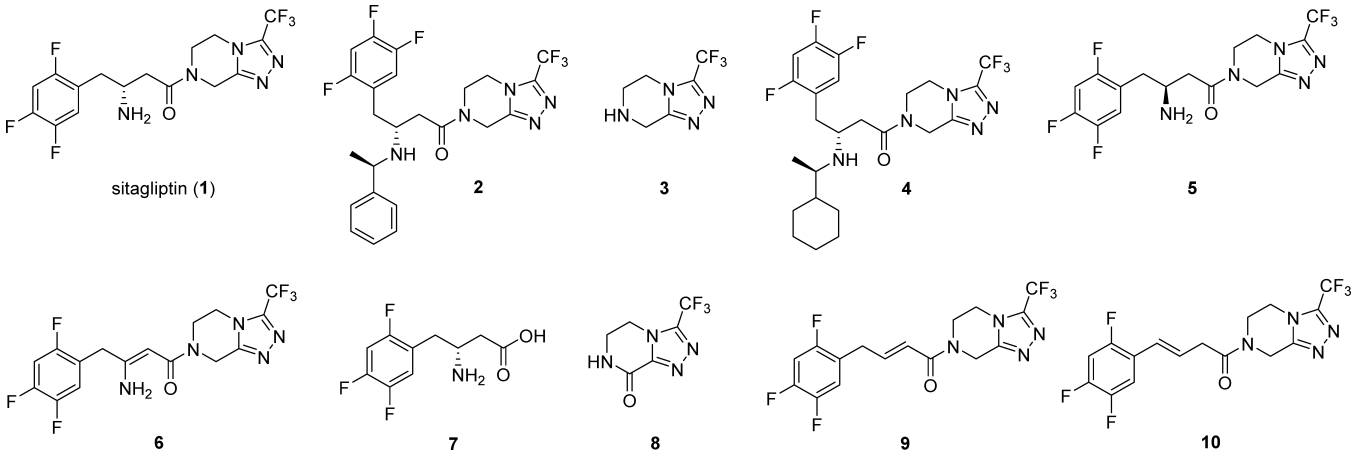

Figure 1. Sitagliptin (**1**) and its main impurities **2**−**10**.

Scheme 1. Our Synthetic Approach for Preparation of Alkene Impurities I (9) and II (10) via the Intermediate 12

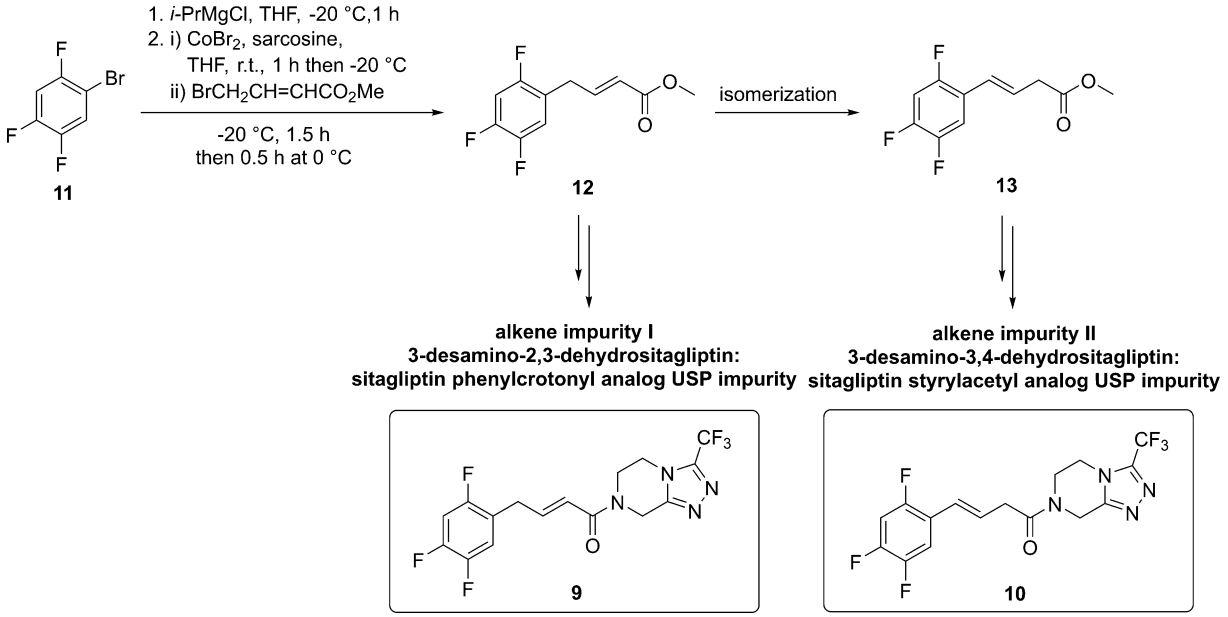

synthesis.[4] Other impurities reported as sitagliptin intermediates and/or degradation products are enamine impurity **6**, acid impurity **7**, triazole derivative **8**, and two alkene derivatives **9** (3-desamino-2,3-dehydrositagliptin; also known as United States Pharmacopeia (USP) sitagliptin phenylcrotonyl analogue impurity) and **10** (3-desamino-3,4-dehydrositagliptin; also known as UPS sitagliptin styrylacetyl analogue impurity). Compounds **9** and **10** are specified impurities with limits of NMT 0.2% in the United States Pharmacopeia monograph for sitagliptin tablets.[8] Acid impurity **7** was reported as a product of hydrolysis[4] as well as a degradation product,[6,7a] whereas impurities **8**−**10** are degradation related impurities (DRIs) that occur as a result of the degradation processes.[6,7a] Furthermore, alkene impurity **9** is also a process-related impurity formed by acid-catalyzed elimination of amine during the hydrogenolysis reaction.[4]

Some synthetic routes for impurities **2**, **3**, **5**, **6**, **7**, **9**, and **10** were reported in the scientific[4,9] and patent[10−15] literatures, whereas recently identified cyclohexyl impurity **4** was synthesized by Bandichhor and co-authors.[4] Interestingly, synthesis of impurity **9** was reported mainly starting from sitagliptin or late stage intermediates,[4,10] while only one four-step synthetic procedure from 2,4,5-trifluorophenylacetic acid was reported in a Chinese patent application.[12] Furthermore, two additional steps are needed if 2,4,5-trifluorophenylacetic acid is prepared from readily available 1,2,4,5-tetrafluorobenzene.[16] Similarly, the synthesis of alkene impurity **10** was mentioned only in the patent literature;[11,14,15] however, the starting materials were only late stage sitagliptin intermediates or sitagliptin. The aim of our study was thus to develop an efficient and straightforward synthetic route to alkene impurity **10** from a simple, readily available, and cheap starting material. Furthermore, we also considered the preparation of alkene impurity **9** by developing a novel, concise, and high-yielding procedure.

RESULTS AND DISCUSSION

According to the context described above, our goal was to develop the most convenient synthetic routes to alkene impurities **9** and **10** from readily available starting materials such as fluorinated benzene derivatives. In light of our previous studies[17,18] where we presented two synthetic approaches

https://dx.doi.org/10.1021/acsomega.9b04393
ACS Omega 2020, 5, 5356−5364

Table 1. Optimization of Reaction Conditions for Hydrolysis of 12 to 14

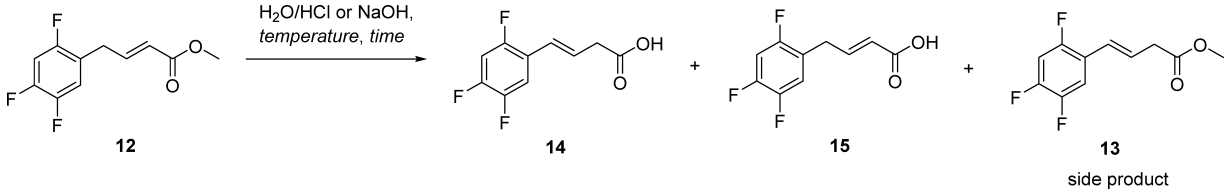

entry	solvent[a]	time (h)	temperature	molar ratio 14/15/13[b]
1	0.2 M NaOH	0.5	r.t.	1:0.46:0.16
2	0.2 M NaOH	24	r.t.	1:0.30:0.02
3	0.2 M NaOH	168	r.t.	1:0.27:0
4	1 M NaOH	0.5	r.t.	1:0.20:0.12
5	1 M NaOH	24	r.t.	1:0.12:0.04
6	3 M NaOH	0.5	r.t.	1:0.16:0.10
7	3 M NaOH	24	r.t.	1:0.13:0.04
8	3 M NaOH	72	r.t.	1:0.10:0.04
9	3 M NaOH	168	r.t.	1:0.20:0
10	3 M NaOH	0.5	100 °C	1:0.16:0.06
11	3 M HCl	0.5	r.t.	NR[c]
12	3 M HCl	24	r.t.	NR[c]
13	3 M HCl	3	100 °C	0.07:1:0

[a]Reaction conditions: **12** (1.0 mmol), 1,4-dioxane (5 mL), solvent (5 mL), time (0.5−168 h), temperature (room temperature (r.t.) or reflux (100 °C)). [b]Calculated by NMR analysis. [c]NR: no reaction occurred, only **12** detected.

using cobalt- or iron-catalyzed cross-coupling reaction, we decided to use the cobalt-catalyzed reaction for the preparation of methyl (*E*)-4-(2,4,5-trifluorophenyl)but-2-enoate (**12**) as our key intermediate.[18] It was synthesized in a one-step reaction from 1-bromo-2,4,5-trifluorobenzene (**11**), which was converted to the corresponding arylmagnesium bromide using isopropylmagnesium chloride as a Grignard exchange reagent. After, aryl Grignard reagent reacted further with methyl 4-bromocrotonate under cobalt-catalyzed cross-coupling reaction to obtain methyl (*E*)-4-(2,4,5-trifluorophenyl)but-2-enoate (**12**) in a 91% yield on a 17 g scale (Scheme 1).

Our first attempt to develop a synthetic route to alkene impurity **10** from methyl (*E*)-4-(2,4,5-trifluorophenyl)but-2-enoate (**12**) was to perform regio-isomerization of allylbenzene intermediate **12** to the regio-isomerized product **13** (Scheme 1). Previous studies have indicated that bases, such as NH_3,[19] LiO*t*Bu,[20] LiHMDS,[21] K_2CO_3,[22,23] KF,[24−26] KOH,[25] and KO*t*Bu,[25,27] can promote the regio-isomerization of the allylbenzene derivative. Accordingly, the conversion of **12** to **13** in the presence of different bases (NaH, Et_3N, NMM, and DBU) was monitored by NMR (see the Supporting Information, Table S1). The results revealed that the best ratio of **12**/**13** was 0.23:1, which was obtained with NMM (10 equiv.) after a 72-h reaction time (Table S1, entry 9). Additionally, the use of NaOH as a base was also examined; however, regio-isomerization along with the hydrolysis of methyl ester occurred. Nevertheless, acid **14** was obtained in high yield (Table 1), which prompted us to synthesize the alkene impurity **10** by using the coupling reaction between the acid **14** and amine **3**. On the other hand, the acid-catalyzed hydrolysis led only to unisomerized acid **15** (Table 1). Therefore, we decided to incorporate hydrolysis of methyl ester **12** to corresponding acids **15** and **14** for the syntheses of both alkene impurities **9** and **10**, respectively.

In a continuation of our study, we optimized the hydrolysis of methyl ester **12** to acids **14** and **15** with regard to the reaction time, temperature, and amount of base used (Table 1). In the case of NaOH, the main challenge was to obtain fully regio-isomerized acid **14** without the presence of unisomerized acid **15** or unhydrolyzed regio-isomerized methyl ester **13**. A prolonged reaction time and low molarity of NaOH did not circumvent this problem (Table 1, entries 1−3). Increasing the molarities of used NaOH to 1 and 3 M provided better selectivity and lowered the formation of **15** and **13** (Table 1, entries 4−8). Furthermore, heating and a shorter reaction time also did not improve the ratio (Table 1, entry 10). In the end, the optimal reaction conditions were obtained when methyl ester **12** was hydrolyzed up to 90% with 3 M NaOH in 24 or 72 h (Table 1, entries 7 and 8). On the other hand, almost complete hydrolysis to **15** occurred by refluxing with 3 M HCl (Table 1, entry 13), whereas no product **15** was detected at room temperature (Table 1, entries 11 and 12). To sum up, acid-catalyzed hydrolysis led to almost quantitative conversion of ester **12** to acid **15**, whereas in basic condition hydrolysis of an ester **12** concomitant with regio-isomerization reaction to acid **14** occurred. However, regio-isomerization did not occur quantitatively (the most optimal ratio was 1:0.10 as shown in Table 1, entry 8) despite the use of concentrated basic solutions and a prolonged reaction time.

With the appropriate reaction conditions for the preparation of acid derivatives **14** and **15** in hand, the next focus was on the screening of different activating reagents for their use in the construction of title compounds **9** and **10** via coupling with **3**. Two main objectives of optimization had to be monitored carefully, reaction yield and selectivity. It was found that compound **9** is prone to regio-isomerization to **10** under the reaction conditions and/or workup. Because both compounds have similar physico-chemical properties, they were difficult to separate completely by column chromatography. Selectivity of reaction conditions was thus highly important. Therefore, we decided to test two different approaches to find the optimal selectivity: a coupling reagent approach and acid activation via

https://dx.doi.org/10.1021/acsomega.9b04393
ACS Omega 2020, 5, 5356−5364

Table 2. Base Screening for Amidation to Alkene Impurity I (9)

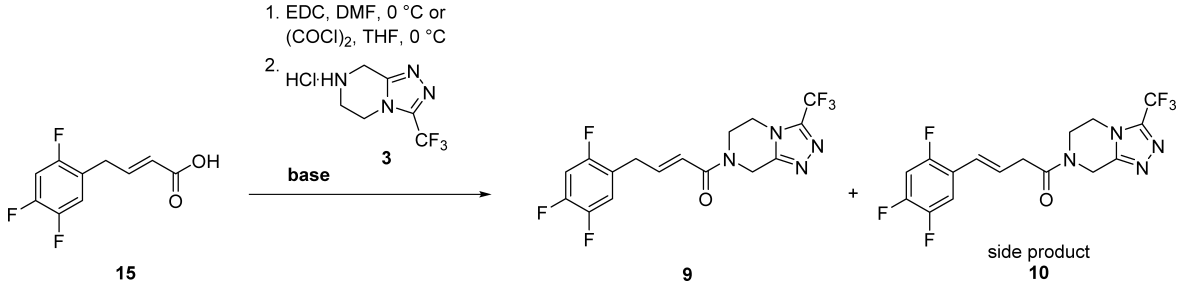

entry	base[a]	activating reagent	time(h)	temperature	overall yield[a,b] **9** + **10** (%)	selectivity ratio **9**:**10**[c]
1	NMM	EDC	1	0 °C	53	31.9
2	NMM	EDC	2	r.t.	77	30.4
3	Et_3N	EDC	1	0 °C	67	17.5
4	Et_3N	EDC	2	r.t.	61	15.5
5	Py	EDC	2	r.t.	43	26.2
6	DMAP	EDC	2	r.t.	39	11.1
7	NMM/DMAP = 9/1	EDC	1	0 °C	85	20.5
8	NMM/DMAP = 9/1	EDC	2	r.t.	75	17.0
9	NMM/DMAP = 1/1	EDC	1	0 °C	57	15.8
10	NMM/DMAP = 1/1	EDC	2	r.t.	54	14.8
11	NMM/Py = 1/1	EDC	1	0 °C	44	18.9
12	NMM/Py = 1/1	EDC	2	r.t.	42	18.7
13	NMM[b]	$(COCl)_2$	1	0 °C	84	30.8
14	Et_3N[b]	$(COCl)_2$	1	0 °C	91	23.6
15	Py[b]	$(COCl)_2$	2	0 °C	70	13.4

[a]Reaction conditions by coupling reagent method: (i) **15** (0.50 mmol, 0.108 g), DMF (5 mL), 0 °C, EDC × HCl (0.50 mmol, 0.096 g), 0.5 h; (ii) **3** × HCl (0.5 mmol, 0.114 g), base (0.5 mmol), 0 °C for 1 h, then r.t. for 1 h. By acid chloride method: (i) **15** (0.46 mmol, 0.10 g), CH_2Cl_2, oxalyl chloride (0.92 mmol, 0.079 mL), DMF (cat.), 0 °C, 1.5 h; (ii) **3** × HCl (0.46 mmol, 0.105 g), base (0.92 mmol), THF (5 mL), 0 °C, 1 h. [b]Determined by HPLC.

an oxalyl chloride (acid chloride) approach. The most common coupling reagents such as DCC (*N*,*N*′-dicyclohexylcarbodiimide), EDC (1-ethyl-3-(3-dimethylaminopropyl)-carbodiimide), TBTU (2-(1*H*-benzotriazole-1-yl)-1,1,3,3-tetramethylaminium tetrafluoroborate), DPPA (diphenylphosphoryl azide), and CDI (1,1′-carbonyldiimidazole) were examined in the presence of NMM (*N*-methylmorpholine) in this study (Table S2), and the overall yield and selectivity ratio were determined by HPLC analysis. The conducted screening of above mentioned coupling methods and coupling reagents demonstrated that the best results are obtained when **15** was activated with oxalyl chloride in CH_2Cl_2 in the presence of a catalytic amount of DMF at 0 °C for 1.5 h followed by the addition of **3** × HCl and NMM in MeCN at 0 °C and stirring for 1 h. This procedure afforded an 88% overall yield of **9** + **10** with a **9**/**10** ratio of 7.8 (Table S2, entry 19). Among all coupling reagents, the best performance in terms of selectivity was noted for EDC, which afforded a 61% overall yield of **9** + **10** with a **9**/**10** ratio of 16 (Table S2, entry 5).

Our next goal was to select the most appropriate solvent for coupling reaction between **15** and **3** using EDC as a coupling reagent in the presence of NMM. Our previous experiments demonstrated that the longer reaction time did not improve the overall yield of product **9**; therefore, only two different reaction times were examined (1 h at 0 °C or the first hour at 0 °C and the second hour at room temperature, see Table S3). When coupling reactions of **15** and **3** with EDC were conducted, DMF was selected as the most optimal solvent with a 77% yield and selectivity ratio of 30.4 (Table S3, entry 10). In the case of the acid activation approach, THF was the most optimal solvent leading to promising an 84% yield and 30.8 selectivity ratio (Table S3, entry 13).

The most important part of the optimization process was the selection of the appropriate base since it could lead to the regio-isomerization of **9** to **10**. In fact, NMR study in deuterated DMF (Figure S15) and THF (Figure S16) revealed that compound **9** undergoes regio-isomerization to **10** when treated with an organic base, such as NMM or Et_3N. The regio-isomerization was observed at 0 °C as well as at room temperature where the equilibrium ratio of **9**/**10** is 1:4 or 1:6.14 after 24 h in deuterated DMF or THF, respectively (Figures S15 and S16). Our further NMR study by 2D NMR techniques (see the Supporting Information, Figures S4 and S11) in $CDCl_3$ showed that the identification of **9** versus **10** or vice versa can be proved by heteronuclear multiple bond correlation (HMBC).

The addition of a base was necessary to form the free base of **3** that would be capable of coupling reactions with **14** and **15**. In addition, the HCl salt of **3** was not soluble in most organic solvents. Different bases such as NMM, Et_3N, pyridine, and DMAP were screened, which resulted in large differences in terms of yields and selectivities in both reactions, with EDC and oxalyl chloride (Table 2). Et_3N (Table 2, entries 3 and 4) was slightly less appropriate compared to NMM (Table 2, entries 1 and 2) when EDC was used, whereas pyridine and DMAP (Table 2, entries 5 and 6) led to lower yields and worse selectivities. The combinations of bases NMM and DMAP (Table 2, entries 7−10) improved the yield and retained good selectivity only when a 9:1 mixture was used (Table 2, entry 7). On the other hand, NMM and Py combination gave less

https://dx.doi.org/10.1021/acsomega.9b04393
ACS Omega 2020, 5, 5356−5364

Scheme 2. Our final Optimized 3-Step Synthetic Approach for Preparation of Alkene Impurities I (9) and II (10) from Readily Available 1-Bromo-2,4,5-trifluorobenzene (11)

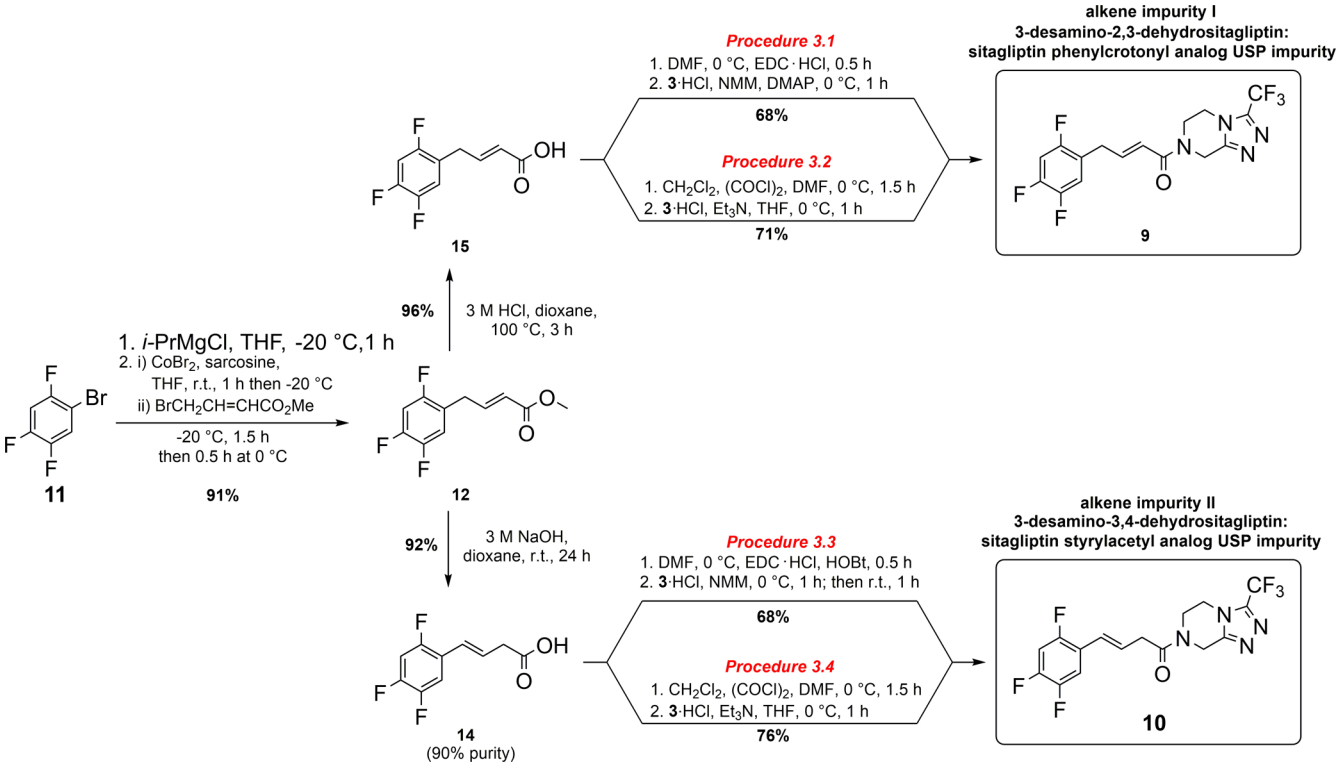

optimal outcomes (Table 2, entries 11 and 12). According to this study, it could be seen that the selection of a base is the most critical step for the selective preparation of amide **9**. The use of NMM with 10% of DMAP as a base and also a catalyst improved the yield to 85%, preserving the good selectivity ratio about 20:1. In the case of activation of carboxylic acid with oxalyl chloride (Table 2, entries 13−15), Et_3N was selected as the most optimal base giving a 91% yield and 23.6 selectivity ratio (Table 2, entry 14).

Our study indicated that the addition of a base favors regio-isomerization of the allylbenzene derivative leading to the more stable isomerized alkene derivative, such as compound **13**, **14**, or **10**. Therefore, the reaction of isomerized acid **14** to alkene impurity **10** is much less problematic in terms of selectivity. Moreover, the addition of a base will favor the formation of isomerized alkene impurity **10**. With the appropriate reaction conditions for amidation of **15** to alkene impurity I (**9**) in hand, we decided to use the optimized oxalyl chloride/Et_3N procedure for conversion of **14** to alkene impurity II (**10**), which was then isolated in a high 76% yield. Furthermore, we also decided to examine the amidation of **14** using EDC as a coupling reagent. Since EDC/HOBt combination gave a higher yield and favorized the formation of **10** over **9** compared to EDC (Table S2, entries 4−9), we used the EDC/HOBt/NMM procedure for the final step of the synthesis of **10**, which was obtained in a satisfactory 68% yield. Thus, we proved that the acid chloride method is more suitable for the last step of the syntheses of both alkene impurities **9** and **10** (Scheme 2).

CONCLUSIONS

In this study, we established two new straightforward and efficient synthetic approaches to two important USP impurities of sitagliptin: 3-desamino-2,3-dehydrositagliptin **9** and 3-desamino-3,4-dehydrositagliptin **10**. These impurities can be generated during the manufacturing process of sitagliptin or the shelf-life of sitagliptin-based drug products. Even though the syntheses of impurities **9** and **10** were already described in the literature and patents[4,9−15] prior our work, our novel synthetic approach starts from the commercially available and most importantly cheap starting material 1-bromo-2,4,5-trifluorobenzene (**11**), which is converted to **9** or **10** in only three steps with satisfactory overall yields ranging from 57 to 64% and purity above 95%. The key reaction was the amide bond formation where the challenging regio-isomerization as a side reaction occurred. Our study indicated that the selection of a base has a high impact on the levels of formation of a side product **10**, thus presenting the most critical feature for selective synthesis of compound **9**. The highest yield (71%) with a satisfactory selectivity ratio of isolated product **9** was obtained using **15**, oxalyl chloride, and Et_3N as a base at 0 °C. On the other hand, the reaction of regio-isomerized acid **14** to alkene impurity **10** is less problematic in terms of selectivity, resulting in a 68 or 76% yield for the EDC/HOBt or acid chloride method, respectively.

To sum up, our work provides facile and reliable access to two key USP impurities that could be used as analytical standards and thereby enables reliable quality control of important antidiabetic drug sitagliptin. Finally, we believe that our work clearly demonstrates the importance of proper selection of solvent, base, and coupling/activating reagents to minimize the carbon−carbon double bond regio-isomerization when Michael acceptor-type allylbenzene derivatives are subjected to amide bond formation.

https://dx.doi.org/10.1021/acsomega.9b04393
ACS Omega 2020, 5, 5356−5364

EXPERIMENTAL SECTION

General Information. All reagents and solvents purchased commercially (from Sigma-Aldrich, Acros Organics, Apollo Scientific, TCI, ABCR GmbH & Co) were used without further purification unless noted otherwise. Tetrahydrofuran was distilled over sodium and dichloromethane was distilled over calcium hydride. Other anhydrous solvents (acetonitrile, DMF) were purchased from Sigma-Aldrich and used without further purification. The reactions with anhydrous solvents were performed in oven-dried glasswares under an argon atmosphere. Melting points were determined on a Reichert micro-hot-stage apparatus and are uncorrected. Thin-layer chromatography (TLC) analysis was performed on silica-gel plates (Merck DC Silica plates 60 GF254). Visualization of compounds was done by illumination with a UV lamp (254 nm). Flash column chromatography was performed on Merck silica gel 60 (mesh size, 70−230), using the indicated solvents. ^{1}H and ^{13}C spectra were recorded with a Bruker Avance III 400 MHz NMR (400 and 100 MHz) instrument at 295 K. Proton spectra were referenced to the signal of $CDCl_3$ (7.26 ppm) or DMSO-d_6 (2.50 ppm). Carbon chemical shifts were determined relative to the ^{13}C signal of $CDCl_3$ (77.16 ppm) or DMSO-d_6 (39.52 ppm). Assignments of some proton and carbon resonances were performed by 2D NMR techniques (^{1}H−^{1}H *gs*-COSY, ^{1}H−^{13}C *gs*-HSQC, and ^{1}H−^{13}C *gs*-HMBC). Coupling constants (J) are given in hertz (Hz). Multiplicities are indicated as follows: s, singlet; d, doublet; dd, double doublet; td, triple doublet; t, triplet; dt, double triplet; ddd, double of doublet of doublet; m, multiplet; and br, broadened. HPLC chromatograms of pure compounds **9** and **10** were recorded on a Thermo Scientific Dionex UltiMate 3000 with a UV detector (254 nm) equipped with an Agilent Extend C18 column (3.5 μm, 4.6 × 150 mm), a flow rate of 1.5 mL/min, an inj. volume of 20 μL, at 25 °C, and an eluent system of H_2O (A) and CH_3CN (B). The following gradient was applied: 0−20 min, 10 → 100% B. Isocratic mixture of CH_3CN 35% and H_2O 65% was used for the analyses of the reaction mixtures via HPLC, with a flow rate of 1 mL/min, and a column temperature of 25 °C. Peak areas of liquid chromatogram were monitored and determined at 254 nm. The reaction yield was calculated in the reference to the known concentration of acetanilide as a standard. Sample preparation: 50 μL of reaction mixture was diluted with 950 μL of acetanilide solution in acetonitrile. The sample was further diluted (1/10) with acetonitrile and filtered to obtain the final sample for HPLC analysis.

Optimized Synthetic Procedures for Alkene Impurities 9 and 10. Synthesis of methyl (*E*)-4-(2,4,5-trifluorophenyl)but-2-enoate (**12**): a dry and nitrogen-flushed flask equipped with a magnetic stirrer and a rubber septum was charged with anhydrous THF (36 mL) and cooled to −20 °C. 1-Bromo-2,4,5-trifluorobenzene (**11**) (25.0 g, 118.5 mmol; 13.9 mL) was introduced through a septum, followed by the dropwise addition (addition rate: 0.666 mL/min) of *i*-PrMgCl (118.5 mmol, 59.25 mL; 2.0 M solution in THF). The reaction mixture was stirred at −20 °C for an additional 1 h. The solution of (2,4,5-trifluorophenyl)magnesium chloride obtained was immediately used further.

A flame-dried and nitrogen-flushed flask equipped with a stirring bar and a rubber septum was charged with $CoBr_2$ (anhydrous, beads, 1.0 g, 4.57 mmol), sarcosine (dried 16 h under vacuum at 50 °C, 8.46 mmol, 0.754 g) and dissolved in anhydrous THF (564 mL) under an argon atmosphere. After 1 h, the reaction mixture was cooled to −20 °C, and methyl 4-bromocrotonate (15.15 g, 84.63 mmol, 10.0 mL) was added. After 15 min, the prepared solution of (2,4,5-trifluorophenyl) magnesium chloride (118.5 mmol, 109 mL) was added dropwise (addition rate: 1.387 mL/min), and the solution obtained was stirred for 1.5 h at −20 °C and an additional 0.5 h at 0 °C. Afterward, the saturated ammonium chloride solution (300 mL) was added to the reaction mixture, which was further washed with ethyl acetate (2 × 500 mL). The combined organic phases were washed with brine (250 mL), dried with anhydrous Na_2SO_4, filtered, and evaporated. The oil residue was purified by flash column chromatography using diethyl ether/petroleum ether (1:10) as a mobile phase to obtain methyl (*E*)-4-(2,4,5-trifluorophenyl)but-2-enoate (**12**) (17.68 g, 91%) as a colorless oil.[17,18] ^{1}H NMR (400 MHz, $CDCl_3$): δ (ppm) 3.45 (d, J = 6.7 Hz, 2H), 3.69 (s, 3H), 5.78 (dtd, J = 15.6, 1.7, 0.5 Hz, 1H), 6.86−7.00 (m, 3H). ^{13}C NMR (100 MHz, $CDCl_3$): δ (ppm) 30.85 (d, J = 2.5 Hz), 51.59, 105.65 (ddd, J = 28.1, 20.7, 0.7 Hz), 118.31 (ddd, J = 19.2, 5.8, 1.3 Hz), 121.09 (ddd, J = 18.5, 5.5, 4.3 Hz), 122.91, 144.65, 146.82 (ddd, J = 244.9, 12.5, 3.7 Hz), 149.04 (ddd, J = 250.3, 14.4, 12.3 Hz), 155.83 (ddd, J = 245.2, 9.4, 2.8 Hz), 166.52.

Synthesis of (*E*)-(2,4,5-trifluorophenyl)but-3-enoic acid (**14**): methyl (*E*)-4-(2,4,5 trifluorophenyl)but-2-enoate (**3**) (21.7 mmol, 5.0 g) was dissolved in 1,4-dioxane (100 mL), 3 M NaOH (100 mL) was added, and then the reaction mixture was stirred at room temperature for 24 h. The solution was washed with diethyl ether (2 × 50 mL), and the water phase was acidified to pH 1 and extracted with diethyl ether (4 × 50 mL). Combined organic phases were washed with brine (100 mL), dried with anhydrous sodium sulfate, filtered, and evaporated to obtain 4.30 g (92%) of a crude oil product, which contained about 90% of **14** and 10% of **15**. The crude product was used in the next reaction without further purification. For **14**: ^{1}H NMR (400 MHz, $CDCl_3$): δ (ppm) 3.33 (d, J = 7.1 Hz, 2H), 6.25−6.32 (m, 1H), 6.57 (d, J = 16.1 Hz, 1H), 6.87−6.93 (m, 1H), 7.23−7.30 (m, 1H), 10.24 (br s, exchanged, 1H). ^{13}C NMR (100 MHz, $CDCl_3$): δ (ppm) 37.89, 105.54 (dd, J = 28.4, 20.9 Hz), 114.37 (dd, J = 19.8, 5.0 Hz), 121.11 (ddd, J = 14.5, 5.8, 4.3 Hz), 123.99 (m), 125.09 (dd, J = 4.0, 2.4 Hz), 146.87 (ddd, J = 244.0, 13.0, 3.5 Hz), 149.12 (ddd, J = 251.7, 14.6, 12.6 Hz), 154.84 (ddd, J = 248.3, 9.1, 2.3 Hz), 174.53. ESI-HRMS ([M + H]$^+$, m/z): Calcd for $C_{10}H_8O_2F_3$, 217.04709; found, 217.04695; ([M-H]$^-$, m/z): Calcd for $C_{10}H_6O_2F_3$, 215.03254; found, 215.03207.

Synthesis of (*E*)-(2,4,5-trifluorophenyl)but-2-enoic acid (**15**): methyl (*E*)-4-(2,4,5-trifluorophenyl)but-2-enoate (**12**) (21.7 mmol, 5.0 g) was dissolved in 1,4-dioxane (50 mL), 3 M HCl (50 mL) was added, and then the reaction mixture was slowly heated to reflux (around 100 °C). The reaction was monitored by TLC (if needed, an additional amount of concentrated HCl was added). Usually, after 3 h heating at 100 °C, the ester hydrolyzed. During the evaporation of 1,4-dioxane, a white solid was formed. Approximately 50 mL of azeotropic mixture was evaporated, the remaining suspension was cooled to 0 °C, and the solid was filtered off and dried to obtain 4.50 g (96%) of **15**. Mp 95−98 °C (water/dioxane). ^{1}H NMR (400 MHz, $CDCl_3$): δ (ppm) 3.52 (d, J = 6.6 Hz, 2H), 5.80 (dt, J = 15.6, 1.4 Hz, 1H), 6.91−7.02 (m, 2H), 7.11 (dt, J = 15.6, 6.6 Hz, 1H), 11.02 (br s, exchanged, 1H); the spectrum is in accordance with literature data.[28] ^{13}C NMR (100 MHz, DMSO-d_6): δ (ppm) 30.15, 105.96 (dd, J = 28.8, 21.2 Hz),

https://dx.doi.org/10.1021/acsomega.9b04393
ACS Omega 2020, 5, 5356−5364

118.82 (dd, J = 19.4, 6.0 Hz), 122.08 (ddd, J = 18.5, 5.7, 4.5 Hz), 123.38, 144.71, 146.06 (ddd, J = 242.3, 12.5, 3.6 Hz), 148.14 (ddd, J = 247.1, 14.0, 13.1 Hz), 155.55 (ddd, J = 243.6, 9.9, 2.3 Hz), 166.82.

Final Optimized Procedures for Amidation to (*E*)-1-(3-(Trifluoromethyl)-5,6-dihydro-[1,2,4]triazolo[4,3-a]-pyrazin-7(8*H*)-yl)-4-(2,4,5-trifluorophenyl)but-2-en-1-one (Alkene Impurity I, 9). Procedure 3.1 (EDC, NMM/DMAP): (*E*)-(2,4,5-trifluorophenyl)but-2-enoic acid **15** (5.0 mmol, 1.08 g) was dissolved in anhydrous DMF (50 mL) and cooled to 0 °C. EDC × HCl (5.25 mmol, 1.006 g) was added, and the reaction was stirred at 0 °C for 0.5 h. Afterward, **3** × HCl (5.0 mmol, 1.14 g), NMM (4.5 mmol, 0.495 mL), and DMAP (0.5 mmol, 0.061 g) were added. The resulting reaction mixture was stirred for 1 h at 0 °C. To the reaction mixture, ethyl acetate (200 mL) was added and washed with 10% citric acid (2 × 100 mL), water (100 mL), and brine (100 mL). The organic phase was evaporated, and the oily residue was purified by gradient flash column chromatography (mobile phases: 1 to 8% of MeOH in diethylether) to obtain 1.32 g (68%) of **9** as a colorless oil.

Procedure 3.2 (oxalyl chloride, Et_3N): (*E*)-(2,4,5-trifluorophenyl)but-2-enoic acid **15** (5.6 mmol, 1.21 g) was charged with anhydrous CH_2Cl_2 (10 mL) and cooled to 0 °C. Oxalyl chloride (9.5 mmol, 0.81 mL) and three drops of anhydrous DMF were added, and the reaction was stirred at 0 °C for 1.5 h. The solvent was then evaporated and dissolved in anhydrous THF (10 mL). Afterward, the obtained solution was cooled down to 0 °C and quickly added to a precooled (0 °C) solution of **3** × HCl (5.6 mmol, 1.28 g) and Et_3N (11.2 mmol, 1.56 mL) in anhydrous THF (15 mL), which was stirred for 1 h at room temperature prior to the addition. The resulting reaction mixture was stirred for 1 h at 0 °C. To the reaction mixture, ethyl acetate (200 mL) was added and washed with 10% citric acid (2 × 100 mL), water (100 mL), and brine (100 mL). The organic phase was evaporated, and the oil residue was purified by gradient flash column chromatography (mobile phases: 1 to 8% of MeOH in diethyl ether) to obtain 1.55 g (71%) of **9** as a colorless oil.

(*E*)-1-(3-(Trifluoromethyl)-5,6-dihydro-[1,2,4]triazolo[4,3-*a*]pyrazin-7(8*H*)-yl)-4-(2,4,5-trifluorophenyl)but-2-en-1-one (**9**): a colorless oil/gel; ^{1}H NMR (400 MHz, $CDCl_3$): δ (ppm) 3.52 (d, J = 6.6 Hz, 2H), 4.07 (br s, 2H), 4.16−4.18 (m, 2H), 4.98 (s, 2H), 6.24 (dt, J = 15.1, 1.4 Hz, 1H), 6.88−6.94 (m, 1H), 6.95−7.04 (m, 2H). ^{13}C NMR (100 MHz, $CDCl_3$): δ (ppm) 31.35 (d, J = 1.9 Hz), 38.56, 42.61, 43.39, 105.80 (dd, J = 28.1, 20.8 Hz), 118.30 (q, J = 270.5 Hz), 118.36 (dd, J = 19.3, 5.8 Hz), 120.55, 120.99 (ddd, J = 18.3, 5.2, 4.5 Hz), 143.75 (q, J = 40.1 Hz), 144.96, 146.86 (dd, J = 245.1, 12.6, 3.7 Hz), 149.11 (ddd, J = 250.6, 14.3, 12.3 Hz), 149.90, 155.88 (ddd, J = 245.2, 9.3, 2.7 Hz), 165.40. ESI-HRMS ($[M + H]^+$, m/z): Calcd for $C_{16}H_{13}N_4OF_6$, 391.09881; found, 391.09853; ($[M - H]^-$, m/z): Calcd for $C_{16}H_{11}N_4OF_6$, 389.08425; found, 391.08476; HPLC: t_R = 9.20 min (98.3 area % at 254 nm). Spectroscopic data are in accordance with literature.[6]

Final Optimized Procedures for Amidation to (*E*)-1-(3-(Trifluoromethyl)-5,6-dihydro-[1,2,4]triazolo[4,3-a]-pyrazin-7(8*H*)-yl)-4-(2,4,5-trifluorophenyl)but-3-en-1-one (Alkene Impurity II, 10). Procedure 3.3 (EDC/HOBt, 1.2 equiv of NMM): crude (*E*)-(2,4,5-trifluorophenyl)but-3-enoic acid **14** (3.25 mmol, 0.702 g) was dissolved in anhydrous DMF (50 mL) and cooled to 0 °C. EDC × HCl (3.58 mmol, 0.686 g) and HOBt (3.58 mmol, 0.484 g) were added, and the reaction was stirred at 0 °C for 0.5 h. Afterward, **3** × HCl (3.25 mmol, 0.52 g) and NMM (3.9 mmol, 0.43 mL) were added. The resulting reaction mixture was stirred for 1 h at 0 °C and 1 h at room temperature. To the reaction mixture, ethyl acetate (200 mL) was added and washed with 10% citric acid (2 × 100 mL), water (100 mL), and brine (100 mL). The organic phase was evaporated, and the oily residue was purified by gradient flash column chromatography (mobile phases: 1 to 8% of MeOH in diethyl ether) to obtain 0.868 g (68%) of **10** as a white solid.

Procedure 3.4 (oxalyl chloride, Et_3N): crude (*E*)-(2,4,5-trifluorophenyl)but-3-enoic acid **14** (6.2 mmol, 1.35 g) was charged with anhydrous CH_2Cl_2 (10 mL) and cooled to 0 °C. Oxalyl chloride (10.5 mmol, 0.90 mL) and three drops of anhydrous DMF were added, and the reaction was stirred at 0 °C for 1.5 h. The solvent was then evaporated, and the residue dissolved in anhydrous THF (10 mL). Afterward, the obtained solution was cooled down to 0 °C and quickly added to a precooled solution (0 °C) of **3** × HCl (6.2 mmol, 1.42 g) and Et_3N (12.4 mmol, 1.73 mL) in anhydrous THF (20 mL), which was stirred for 1 h at room temperature prior to the addition. The resulting reaction mixture was stirred for 1 h at 0 °C. To the reaction mixture, ethyl acetate (200 mL) was added and washed with 10% citric acid (2 × 100 mL), water (100 mL), and brine (100 mL). The organic phase was evaporated, and the oily residue was purified by gradient flash column chromatography (mobile phases: 1 to 8% of MeOH in diethyl ether) to obtain 1.83 g (76%) of **10** as a white solid.

(*E*)-1-(3-(Trifluoromethyl)-5,6-dihydro-[1,2,4]triazolo[4,3-*a*]pyrazin-7(8*H*)-yl)-4-(2,4,5-trifluorophenyl)but-3-en-1-one (**10**): white solid; Mp 105−107 °C; ^{1}H NMR (400 MHz, $CDCl_3$): δ (ppm) 3.43 (d, J = 6.6 Hz, 2H), 3.99−4.12 (m, 2H), 4.15−4.26 (m, 2H), 4.96 (5.02)* (s + s, 2H), 6.31 (dt, J = 15.9, 6.6 Hz, 1H), 6.52 (d, J = 16.2 Hz, 1H), 6.83−6.90 (m, 1H), 7.20−7.28 (m, 1H). ^{13}C NMR (100 MHz, $CDCl_3$): δ (ppm) 37.69 (37.78)*, 38.28 (41.93)*, 42.71 (39.44)*, 43.32 (43.72)*, 105.80 (dd, J = 28.3, 20.9 Hz), 114.62 (dd, J = 19.7, 4.8 Hz), 118.27 (q, J = 270.7 Hz), 120.95 (m), 124.44 (125.09)*, 125.40, 143.91 (q, J = 39.8 Hz), 144.96, 147.06 (ddd, J = 243.7, 12.7, 3.1 Hz), 149.24 (ddd, J = 244.0, 25.8, 12.9 Hz), 149.60, 155.02 (ddd, J = 248.3, 9.1, 2.4 Hz), 169.39 (169.77)*; *mixture of rotamers. ESI-HRMS ($[M + H]^+$, m/z): Calcd for $C_{16}H_{13}N_4OF_6$, 391.09881; found, 391.09845; ($[M-H]^-$, m/z): Calcd for $C_{16}H_{11}N_4OF_6$, 389.08425; found, 391.08481; HPLC: t_R = 9.47 min (98.7 area% at 254 nm). Spectroscopic data are in accordance with literature.[6]

■ ASSOCIATED CONTENT

Supporting Information

The Supporting Information is available free of charge at https://pubs.acs.org/doi/10.1021/acsomega.9b04393.

^{1}H, ^{13}C, HSQC, and HMBC NMR spectra of compounds **9** and **10**; HPLC chromatograms and MS spectra of compounds **9** and **10**; reaction screening details for regio-isomerization of **12** to **13**; reaction screening details for hydrolysis and regio-isomerization of **12** to **14** and **15**; and reaction screening details for the formation of an amide bond (PDF)

https://dx.doi.org/10.1021/acsomega.9b04393
ACS Omega 2020, 5, 5356−5364

AUTHOR INFORMATION

Corresponding Author

Zdenko Časar − *University of Ljubljana, Faculty of Pharmacy, Ljubljana 1000, Slovenia; Lek Pharmaceuticals, d.d., Sandoz Development Center Slovenia, Ljubljana SI-1526, Slovenia;* orcid.org/0000-0002-6689-3353; Email: zdenko.casar@sandoz.com, Zdenko.Casar@ffa.uni-lj.si

Authors

Matej Sova − *University of Ljubljana, Faculty of Pharmacy, Ljubljana 1000, Slovenia*

Rok Frlan − *University of Ljubljana, Faculty of Pharmacy, Ljubljana 1000, Slovenia*

Stanislav Gobec − *University of Ljubljana, Faculty of Pharmacy, Ljubljana 1000, Slovenia;* orcid.org/0000-0002-9678-3083

Complete contact information is available at: https://pubs.acs.org/10.1021/acsomega.9b04393

Author Contributions

[§]M.S. and R.F. contributed equally to this work. All authors have given approval to the final version of the manuscript.

Notes

The authors declare no competing financial interest.

ACKNOWLEDGMENTS

The authors acknowledge the financial support from the Slovenian Research Agency (research core funding no. P1-0208). This manuscript is dedicated in memoriam to Prof. Dr. Janez Levec (1943-2020); University of Ljubljana, Slovenia and National Institute of Chemistry, Slovenia.

REFERENCES

(1) Kim, D.; Wang, L.; Beconi, M.; Eiermann, G. J.; Fisher, M. H.; He, H.; Hickey, G. J.; Kowalchick, J. E.; Leiting, B.; Lyons, K.; Marsilio, F.; McCann, M. E.; Patel, R. A.; Petrov, A.; Scapin, G.; Patel, S. B.; Roy, R. S.; Wu, J. K.; Wyvratt, M. J.; Zhang, B. B.; Zhu, L.; Thornberry, N. A.; Weber, A. E. (2R)-4-oxo-4-[3-(trifluoromethyl)-5,6-dihydro[1,2,4]triazolo[4,3-*a*]pyrazin-7(8H)-yl]-1-(2,4,5-trifluorophenyl)butan-2-amine: a potent, orally active dipeptidyl peptidase IV inhibitor for the treatment of type 2 diabetes. *J. Med. Chem.* **2005**, *48*, 141−151.

(2) Pathak, R.; Bridgeman, M. B. Dipeptidyl peptidase-4 (DPP-4) inhibitors in the management of diabetes. *Pharm. Ther.* **2010**, *35*, 509−513.

(3) Zhou, L.; Mao, B.; Reamer, R.; Novak, T.; Ge, Z. Impurity profile tracking for active pharmaceutical ingredients: case reports. *J. Pharm. Biomed. Anal.* **2007**, *44*, 421−429.

(4) Metil, D. S.; Sampath, A.; Reddy, J. R.; Chandrashekar, E. R. R.; Dahanukar, V. H.; Reddy, C. V. R.; Bandichhor, R. Efficient and convenient synthetic routes for sitagliptin impurities. *ChemistrySelect* **2018**, *3*, 2723−2729.

(5) (a) Ahuja, S.; Alsante, K. M. *Handbook of isolation and characterization of impurities in pharmaceuticals*; 1st ed.; Ahuja, S., Ed.; Alsante, K. M., Ed.; Academic Press: San Diego, 2003, Volume *5*, pp 119−143. (b) Ahuja, S.; Scypinski, S. *Handbook of modern pharmaceutical analysis*; Volume *10*, 2nd ed.; Ahuja, S., Ed.; Scypinski, S., Ed.; Academic Press: San Diego, 2011; pp 59−169. (c) Schniepp, S. *Overview of USP-NF requirements for stability purposes. In Handbook of stability testing in pharmaceutical development*; Kim, H.-B., Ed.; Springer Science + Business Media: New York, 2009; pp 189−199. (d) Hostyn, S.; Persich, P.; Jhajra, S; Vanhoutte, K. Protocols for characterization of degradation products with special emphasis on mutagenic degradation impurities. In *Methods for stability testing of pharmaceuticals*; Bajaj, S., Ed.; Singh, S., Ed.; Springer Nature: New York, 2018; pp 123−142. (e) Jain, D.; Basniwal, P. K. Forced degradation and impurity profiling: recent trends in analytical perspectives. *J. Pharm. Biomed. Anal.* **2013**, *86*, 11−35. (f) Holm, R.; Elder, D. P. Analytical advances in pharmaceutical impurity profiling. *Eur. J. Pharm. Sci.* **2016**, *87*, 118−135. (g) Görög, S. Critical review of reports on impurity and degradation product profiling in the last decade. *TrAC, Trends Anal. Chem.* **2018**, *101*, 2−16. (h) Olsen, B. A.; Sreedhara, A.; Baertschi, S. W. Impurity investigations by phases of drug and product development. *TrAC, Trends Anal. Chem.* **2018**, *101*, 17−23. (i) Singh, D. K.; Sahu, A.; Kumar, S.; Singh, S. Critical review on establishment and availability of impurity and degradation product reference standards, challenges faced by the users, recent developments, and trends. *TrAC, Trends Anal. Chem.* **2018**, *101*, 85−107. (j) Maggio, R. M.; Calvo, N. L.; Vignaduzzo, S. E.; Kaufman, T. S. Pharmaceutical impurities and degradation products: Uses and applications of NMR techniques. *J. Pharm. Biomed. Anal.* **2014**, *101*, 102−122. (k) Foti, C.; Alsante, K.; Cheng, G.; Zelesky, T.; Zell, M. Tools and workflow for structure elucidation of drug degradation products. *TrAC, Trends Anal. Chem.* **2013**, *49*, 89−99. (l) Popkin, M. E.; Borman, P. J.; Omer, B. A.; Looker, A.; Kallemeyn, J. M. Enhanced approaches to the identification, evaluation, and control of impurities. *J. Pharm. Innov.* **2019**, *14*, 176−184. (m) Roy, J. Pharmaceutical impurities—A mini-review. *AAPS PharmSciTech* **2002**, *3*, 1−8.

(6) Sonune, D. P.; Mone, M. K. Isolation, characterization of degradation products of sitagliptin and development of validated stability-indicating HPLC assay method for sitagliptin api and tablets. *Int. J. Pharm. Sci. Res* **2013**, *4*, 3494−3503.

(7) (a) Farooqui, I.; Kakde, R. B. Reversed-phase liquid chromatography with mass detection and NMR characterization of sitagliptin degradation related impurities. *Int. J. Pharm. Sci. Res.* **2016**, *38*, 4240−4230. (b) Prasad, P. B. N.; Satyanarayana, K.; Krishna, M. G. Impurity profiling and regulatory aspects of sitagliptin active pharmaceutical ingredient. *Int. J. Sci. Res.* **2018**, *7*, 6−11.

(8) U.S. Pharmacopoeia, 2016, *U.S. Pharmacopoeia and National Formulary [USP39−NF34]*, Volume 3, Rockville, Md: United States Pharmacopeial Convention, Inc; 2016. USP monographs, (a) Sitagliptin Phosphate, 5854−5855; (b) Sitagliptin Tablets, 5852−5854.

(9) Bao, H.; Bayeh, L.; Tambar, U. Catalytic enantioselective allylic amination of olefins for the synthesis of *ent*-sitagliptin. *Synlett* **2013**, *24*, 2459−2463.

(10) Janagani, S.; Thaduri, V. K.; Vamaraju, R. Expedient synthesis of sitagliptin and its phosphate hydrate salt. WO2015/120111 A2, 2015.

(11) Peng, F.; Gao, Y.; He, Y.; Wu, Z. Sitagliptin impurity synthesis method. CN105085531 B, 2017.

(12) Gao, Y.; He, Y.; Peng, F.; Wu, Z.; Feng, B. Synthesis method of sitagliptin impurities. CN105130999 A, 2015.

(13) Lai, J.; Kou, J. Preparation method of sitagliptin impurity. CN 104387393 A, 2015.

(14) Zhang, S.; Yang, H.; Ge, J.; Shen, L.; Yang, L.; Wang, L.; Wang, J. Preparation method of sitagliptin phosphate analog I. CN106397444 A, 2015.

(15) Gao, Y.; He, Y.; Peng, F.; Feng, B.; Wu, Z. Method for synthesizing sitagliptin impurity. CN105330664 A, 2016.

(16) Feng, Q.; Xia, X.; Zheng, Y.; Kong, X. Preparation method of 2,4,5-trifluoro phenylacetic acid. CN104418727 A, 2015.

(17) Sova, M.; Frlan, R.; Gobec, S.; Stavber, G.; Časar, Z. D-Glucosamine in iron-catalysed cross-coupling reactions of Grignards with allylic and vinylic bromides: application to the synthesis of a key sitagliptin precursor. *Appl. Organometal. Chem.* **2015**, *29*, 528−535.

(18) Frlan, R.; Sova, M.; Gobec, S.; Stavber, G.; Časar, Z. Cobalt-catalyzed cross-coupling of Grignards with allylic and vinylic bromides: use of sarcosine as a natural ligand. *J. Org. Chem.* **2015**, *80*, 7803−7809.

(19) Qin, L.; Zard, S. Z. Radical-based route to 2-(trifluoromethyl)-1,3,4-oxadiazoles and trifluoromethyl-substituted polycyclic 1,2,4-triazoles and dihydrofurans. *Org. Lett.* **2015**, *17*, 1577−1580.

(20) Lu, X.-Y.; Li, J.-S.; Wang, J.-Y.; Wang, S.-Q.; Li, Y.-M.; Zhu, Y.-J.; Zhou, R.; Ma, W.-J. Cu-catalyzed cross-coupling reactions of vinyl epoxide with organoboron compounds: access to homoallylic alcohols. *RSC Adv.* **2018**, *8*, 41561−41565.
(21) Guha, S. K.; Shibayama, A.; Abe, D.; Sakaguchi, M.; Ukaji, Y.; Inomata, K. "Syn-effect" in the conversion of (*E*)-α,β-unsaturated esters into the corresponding β,γ-unsaturated esters and aldehydes into silyl enol ethers. *Bull. Chem. Soc. Jpn* **2004**, *77*, 2147−2157.
(22) Neumann, R.; Sasson, Y. An evaluation of polyethylene-glycol as a catalyst in liquid-gas phase transfer catalysis: the base-catalyzed isomerization of allylbenzene. *J. Mol. Catal.* **1985**, *33*, 201−208.
(23) al-Maskery, I.; Girling, K.; Jackson, S. D.; Pugh, L.; Spence, R. R. High activity solid base catalysts for alkenyl aromatic isomerisation. *Top. Catal.* **2010**, *53*, 1163−1165.
(24) Radhakrishna, A. S.; Suri, S. K.; Prasad Rao, K. R. K.; Sivaprakash, K.; Singh, B. B. Potassium fluoride on alumina-A versatile reagent for isomerization of olefins. *Synth. Commun.* **1990**, *20*, 345−348.
(25) Ngoc Thach, L.; Lieu Hanh, D.; Ba Hiep, N.; Radhakrishna, A. S.; Singh, B. B.; Loupy, A. Further Improvements in isomerization of olefins in solvent-free conditions. *Synth. Commun.* **1993**, *23*, 1379−1384.
(26) Luu, T. X.; Lam, T.; le, T.; Duus, F. Fast and green microwave-assisted conversion of essential oil allylbenzenes into the corresponding aldehydes via alkene isomerization and subsequent potassium permanganate promoted oxidative alkene group cleavage. *Molecules* **2009**, *14*, 3411−3424.
(27) Cram, D. J.; Uyeda, R. T. Intramolecular proton transfer in a base-catalyzed allylic rearrangement. *J. Am. Chem. Soc.* **1962**, *84*, 4358−4359.
(28) Hayama, N.; Kuramoto, R.; Földes, T.; Nishibayashi, K.; Kobayashi, Y.; Pápai, I.; Takemoto, Y. Mechanistic insight into asymmetric hetero-Michael addition of α,β-unsaturated carboxylic acids catalyzed by multifunctional thioureas. *J. Am. Chem. Soc.* **2018**, *140*, 12216−12225.

https://dx.doi.org/10.1021/acsomega.9b04393
ACS Omega 2020, 5, 5356−5364